

Journal Pre-proof

In-silico Screening and ADMET evaluation of Therapeutic MAO-B Inhibitors against Parkinson Disease

Abduljelil Ajala, Wafa Ali Eltayb, Terungwa Michael Abatyough, Stephen Ejeh, Mohamed El Fadili, Habiba Asipita Otaru, Emmanuel Israel Edache, A. Ibrahim Abdulganiyyu, Omole Isaac Areguamen, Shashank M. Patil, Ramith Ramu

PII: S2949-866X(23)00134-X

DOI: <https://doi.org/10.1016/j.ipha.2023.12.008>

Reference: IPHA 85

To appear in: *Intelligent Pharmacy*

Received Date: 26 November 2023

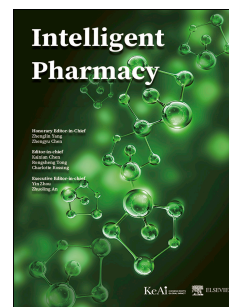
Revised Date: 22 December 2023

Accepted Date: 23 December 2023

Please cite this article as: Ajala A, Eltayb WA, Abatyough TM, Ejeh S, El Fadili M, Otaru HA, Edache EI, Abdulganiyyu AI, Areguamen OI, Patil SM, Ramu R, *In-silico* Screening and ADMET evaluation of Therapeutic MAO-B Inhibitors against Parkinson Disease, *Intelligent Pharmacy* (2024), doi: <https://doi.org/10.1016/j.ipha.2023.12.008>.

This is a PDF file of an article that has undergone enhancements after acceptance, such as the addition of a cover page and metadata, and formatting for readability, but it is not yet the definitive version of record. This version will undergo additional copyediting, typesetting and review before it is published in its final form, but we are providing this version to give early visibility of the article. Please note that, during the production process, errors may be discovered which could affect the content, and all legal disclaimers that apply to the journal pertain.

© 2023 The Authors. Publishing services by Elsevier B.V. on behalf of KeAi Communications Co. Ltd.



AA designed and wrote the manuscript, WAE, ATM, SE, ME, OHA, EIE, AAI, OIA, SMP and RR supervised the research, AA carried out the statistical analysis. All authors read and approved the final manuscript

Journal Pre-proof

(Article)

***In-silico* Screening and ADMET evaluation of Therapeutic MAO-B Inhibitors against Parkinson Disease**

Ajala Abduljelil¹, Wafa Ali Eltayb², Abatyough Terungwa Michael³, Stephen Ejeh¹, Mohamed El Fadili⁴, Otaru Habiba Asipita⁵, Emmanuel Israel Edache⁶, Abdulganiyyu A. Ibrahim⁷, Omole Isaac Areguamen⁸, Shashank M Patil⁹, Ramith Ramu⁹

¹Department of Chemistry, Faculty of Physical Sciences, Ahmadu Bello University, Zaria Nigeria

²Biotechnology Department, Faculty of Sciences and Technology, Shendi University, Shendi 11111, Sudan;

³Chemical sciences department Bingham University, Karu.Nigeria

⁴Engineering Materials, Modeling and Environmental Laboratory, Faculty of Sciences Dhar El Mehraz, Sidi Mohammed Ben Abdellah University, BP 1796 Atlas, Fez 30000, Morocco

⁵Department of Chemistry, Nigerian Defence Academy, Kaduna Nigeria

⁶Faculty of Physical Sciences, Department of Pure and Applied Chemistry, University of Maiduguri

⁷Department of Public and Environmental Health, Federal University Dutse, Jigawa

⁸Department of Applied Chemistry, Federal University, Dutsin-ma Katsina Nigeria

⁹Department of Biotechnology and Bioinformatics, School of Life Sciences, JSS Academy of Higher Education and Research, Mysuru 570015, Karnataka, India

*Correspondence: abdulajala39@gmail.com, Tel: +2348036910413

Abstract: MAOs are flavoenzymes that aid in the oxidative deamination of neurotransmitters such as dopamine, serotonin, and epinephrine. MAO inhibitors are antidepressants that act by inhibiting neurotransmitter breakdown in the brain and controlling mood. MAO inhibitors with the chlorophenyl-chromone-carboxamide structure have been shown in investigations to be extremely effective. The current study employs *in-silico* screening, MD simulation, and drug kinetics evaluation, all of which are evaluated using different criteria. The study comprised 37 ligands, and three stood out as the best, with greater binding scores above the threshold value. Docking analysis found that compound 34 had the highest docking score in the series (-13.60 kcal mol⁻¹) and interacted with the important amino acids TYR 435, CYS 397, CYS 172, PHE 343, TYR 398, and LYS 296 required for MAO inhibitory activity. The ADMET study revealed that the compounds had drug-like properties. The results of this study could be used to develop chromone drugs that target the MAO inhibitor. The top three ligands with the highest force and work were then simulated using molecular dynamics. The protein-ligand complexes had steady trajectories throughout the 100 ns simulation,

according to the data. Furthermore, the drug likeliness predicted by ADMET analysis findings indicated that the top three lead compounds had strong inhibitory efficiency, superior pharmacokinetics, and were non-toxic under physiological settings. As a result, these compounds have the potential to be exploited as possible treatment medications for PD.

Keywords: MAO-B Inhibitors, Parkinsonism Disorder, Molecular Docking, Molecular Dynamics Simulation, Pharmacokinetic.

1. Introduction

Parkinson's disease (PD) is a common neurological abnormality [1]. A combination of hereditary and environmental variables is thought to have a role in aberrant protein aggregation within certain groups of neurons, resulting in cell malfunction and, eventually, death [2]. Given the huge number of Motor and non-motor symptoms constitute a large number of patients in PD [3-5].

Potent adenosine A2a antagonists were employed as prospective anti-Parkinson disease medicines in retrospect, according to a Non-linear QSAR analysis coupled with pharmacophore modelling [6]. Researchers used QSAR modelling to find LRRK2 inhibitors for PD [7]. Munteanu demonstrated in 2010 that Drug Discovery and Design for Complex Diseases Using QSAR Computational Methods [8]. Nikolic employed theoretical Drug design for CNS [9]. De and Roy conducted research on QSAR modelling of PET imaging agents for the diagnosis of PD targeting dopamine receptors in 2020 [10]. Helguera demonstrated in 2013 how different QSAR models might be coupled to improve predictions of human monoamine oxidase inhibitors. The resultant models demonstrated statistical significance, interpretability, and prediction power on an external validation set of chromone derivatives with unknown activity [11]. Following that, Tong et al found that the model has a good and consistent predictive capacity, as well as the molecular docking with proteins target (PDB ID: 5CGJ), ADMET, and drug-likeness prediction performed, which demonstrated appropriate docking score, suitable ADMET, and drug-likeness qualities [12].

There have been major recent advancements in our understanding of the PD's pathophysiology. In addition to the recognized motor problems, there has been a growing recognition that the disease may be associated with major non-motor disturbances [13]. Although there is no cure there are numerous management options for early Parkinson's disease treatment [14]. As the disease develops, more treatment options become available, however, managing PD patients is difficult because pharmacological alternatives are restricted and levodopa remains the backbone of treatment [15]. However, levodopa-induced dyskinesia (LID) is a common side effect reported in PD patients treated with levodopa normally encountered after a long period of treatment [16], but occasionally, this may be seen even after a few days or months of treatment. MAOs are widely distributed enzymes that have a flavin adenine dinucleotide (FAD) cofactor covalently linked to a cysteine residue. They are expressed in a variety of living species and are in charge of key neurotransmitter metabolism in both the central nervous system (CNS) and peripheral tissues [17]. MAO-B is an isoenzyme that binds to the outer mitochondrial membrane and catalyzes the oxidative deamination of aromatic amine substrates. MAO-B principally metabolizes dopamine and phenethylamine, and it is the enzyme's distribution tissue. Because of its role in neurotransmitter metabolism in the cerebrum, MAO-B is a proven therapeutic target for neurological disorders. Furthermore, the expression of MAO-B in neural tissues increases fourfold with age, resulting in increased dopamine metabolism and higher hydrogen peroxide production [18]. Finally, repurposing MAO-targeted medication for PD treatment remains a prospective technique especially, when integrated with *in-silico* techniques and protein target of ID: 6FW0 (crystal structure of human MAO-B in complex with chlorophenyl-chromone-carboxamide). Computer-assisted drug design (CADD) using *in-silico* techniques has been of significant importance and has been reported nowadays in many literatures [19-25]. Computer-assisted drug design (CADD) using *in-silico* techniques has been used in the identification and development of non-toxic, highly effective, and inexpensive drugs for the treatment of PD [26-28].

This research aimed to utilize *In-silico* Screening, MD simulation, and Drug Kinetics Assessment to determine the mechanism of interaction between MAO-B potent inhibitors and protein targets for the treatment of PD by analyzing their binding interactions through molecular simulation and Pharmacokinetic ability.

2. Materials and Methods

Protein Target preparation for docking

The crystal structure of human monoamine oxidase B (MAO B) in complex with chlorophenyl-chromone-carboxamide (PDB ID: 6FW0; chain A) was retrieved from RCSB PDB database (<https://www.rcsb.org/>) as shown in Figure 1. AutoDockTools, v 1.5.6 was utilized in protein preparation [29]. Further, the point of attachment of the protein by the native ligand was unravelled from the research carried out by [30]. Further, tools used in a previous study were used to prepare the ligand [29,31].

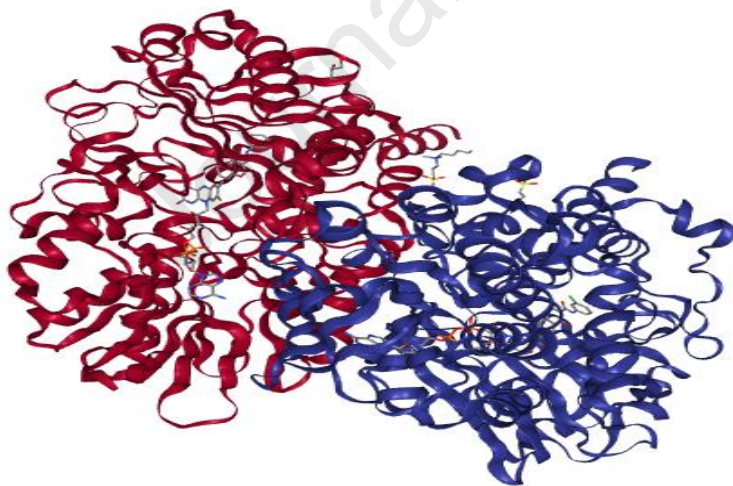


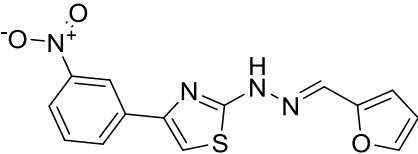
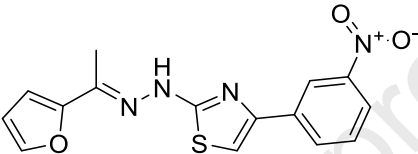
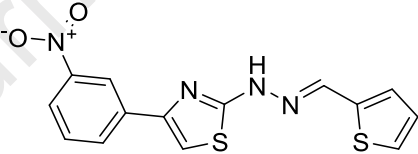
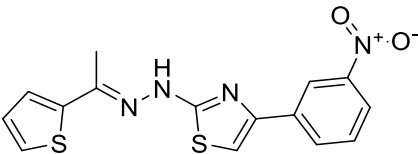
Figure 1: unprepared protein target with code ID 6FW0

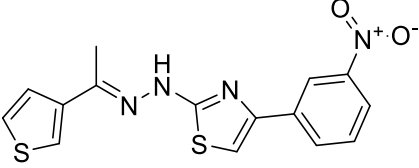
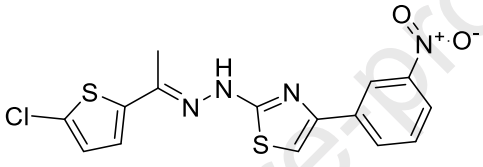
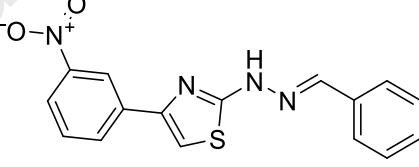
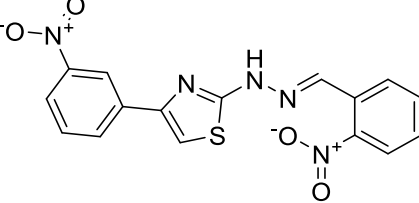
Lead molecules preparation

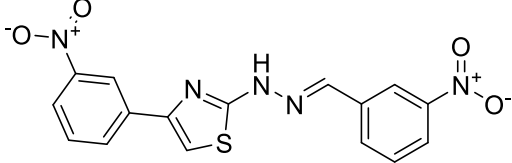
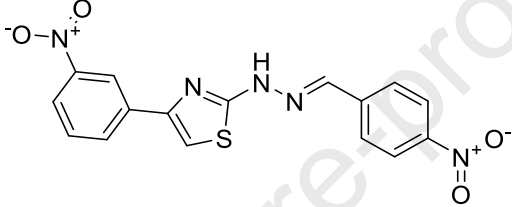
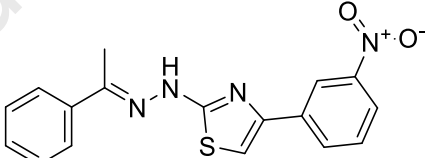
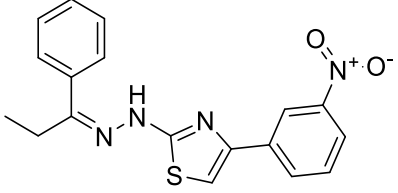
Thirty-seven (37) new series of hydrazone derivatives were taken from the literature [32] which are anti-Parkinson's disease with the chemical structures. ChemDraw was used to draw the chemical compounds, saved in SD file, and further converted to 3-D using the Spartan'14 software as shown in Table-1, and finally saved in PDB format in preparation for docking.

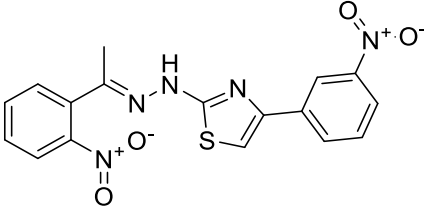
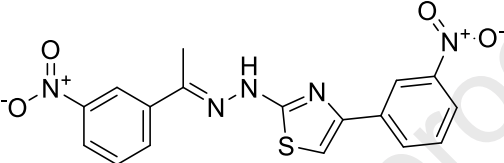
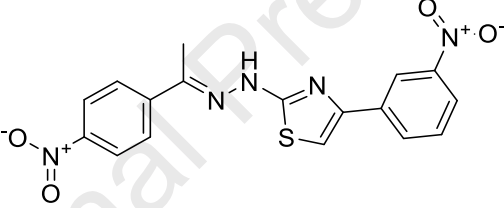
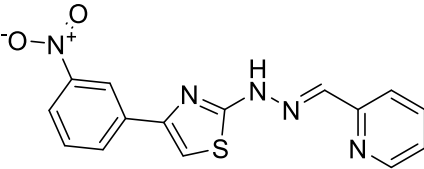
Journal Pre-proof

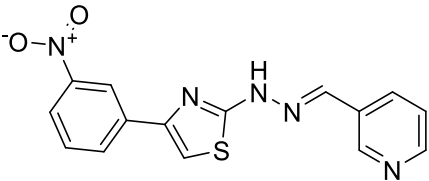
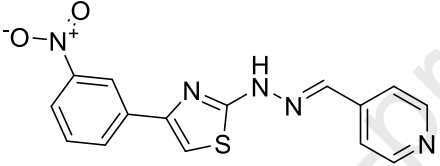
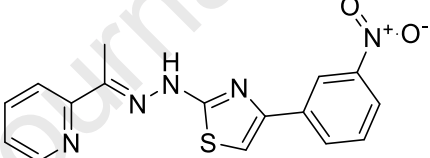
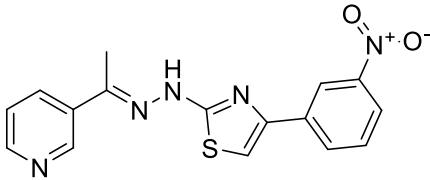
Table 1: 2D structures of chemical compounds

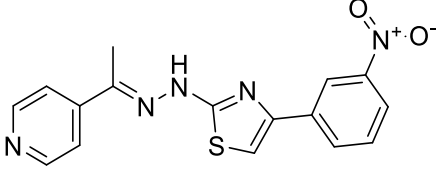
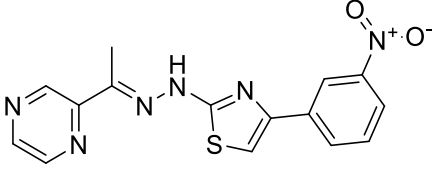
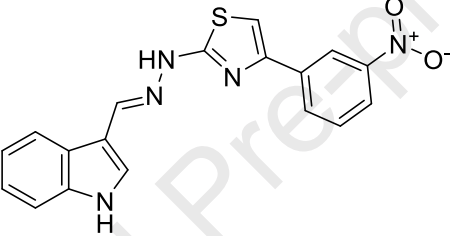
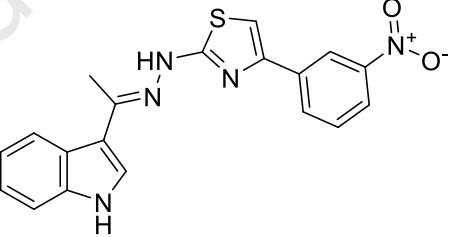
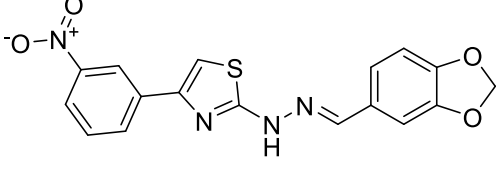
Compound ID	2D structures
1	 <p>(E)-2-(2-(furan-2-ylmethylene)hydrazineyl)-4-(3-nitrophenyl)thiazole</p>
2	 <p>(E)-2-(2-(1-(furan-2-yl)ethylidene)hydrazineyl)-4-(3-nitrophenyl)thiazole</p>
3	 <p>(E)-4-(3-nitrophenyl)-2-(2-(thiophen-2-ylmethylene)hydrazineyl)thiazole</p>
4	 <p>(E)-4-(3-nitrophenyl)-2-(2-(1-(thiophen-2-yl)ethylidene)hydrazineyl)thiazole</p>

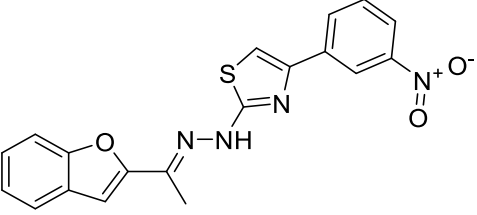
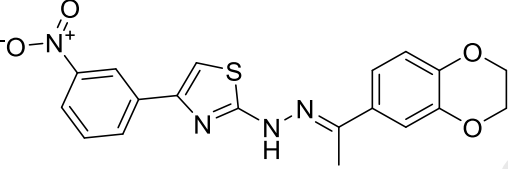
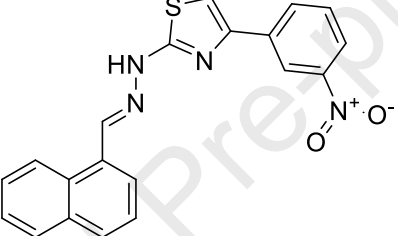
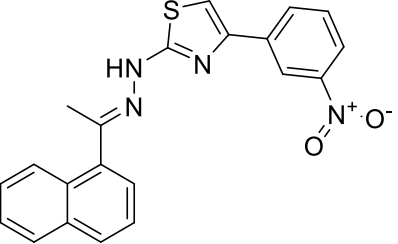
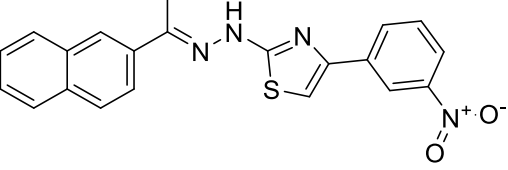
5	 <p>(E)-4-(3-nitrophenyl)-2-(2-(1-(thiophen-3-yl)ethylidene)hydrazineyl)thiazole</p>
6	 <p>(E)-2-(2-(1-(5-chlorothiophen-2-yl)ethylidene)hydrazineyl)-4-(3-nitrophenyl)thiazole</p>
7	 <p>(E)-2-(2-benzylidenehydrazineyl)-4-(3-nitrophenyl)thiazole</p>
8	 <p>(E)-2-(2-(2-nitrobenzylidene)hydrazineyl)-4-(3-nitrophenyl)thiazole</p>

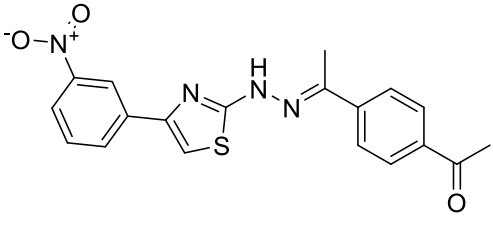
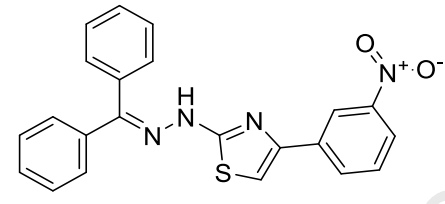
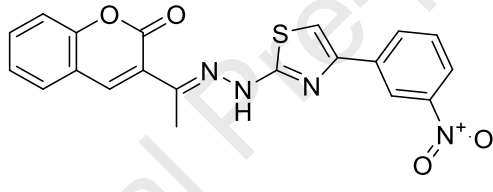
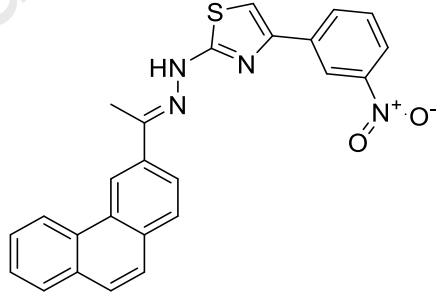
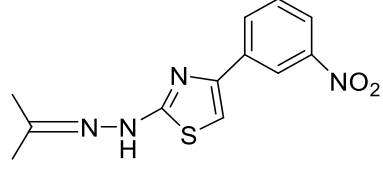
9	 <p>(E)-2-(2-(3-nitrobenzylidene)hydrazineyl)-4-(3-nitrophenyl)thiazole</p>
10	 <p>(E)-2-(2-(4-nitrobenzylidene)hydrazineyl)-4-(3-nitrophenyl)thiazole</p>
11	 <p>(E)-4-(3-nitrophenyl)-2-(2-(1-phenylethylidene)hydrazineyl)thiazole</p>
12	 <p>(Z)-4-(3-nitrophenyl)-2-(2-(1-phenylpropylidene)hydrazineyl)thiazole</p>

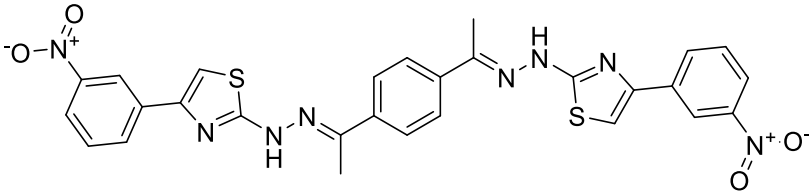
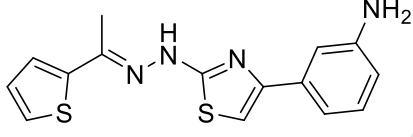
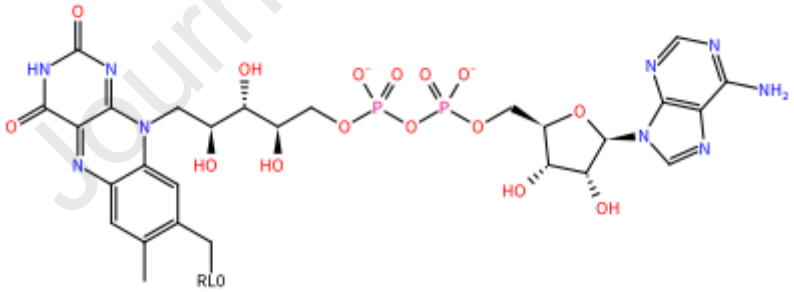
13	 <p>(E)-4-(3-nitrophenyl)-2-(2-(1-(2-nitrophenyl)ethylidene)hydrazineyl)thiazole</p>
14	 <p>(E)-4-(3-nitrophenyl)-2-(2-(1-(3-nitrophenyl)ethylidene)hydrazineyl)thiazole</p>
15	 <p>(E)-4-(3-nitrophenyl)-2-(2-(1-(4-nitrophenyl)ethylidene)hydrazineyl)thiazole</p>
16	 <p>(E)-4-(3-nitrophenyl)-2-(2-(pyridin-2-ylmethylene)hydrazineyl)thiazole</p>

17	 <p>(E)-4-(3-nitrophenyl)-2-(2-(pyridin-3-ylmethylene)hydrazineyl)thiazole</p>
18	 <p>(E)-4-(3-nitrophenyl)-2-(2-(pyridin-4-ylmethylene)hydrazineyl)thiazole</p>
19	 <p>(E)-4-(3-nitrophenyl)-2-(2-(1-(pyridin-2-yl)ethylidene)hydrazineyl)thiazole</p>
20	 <p>(E)-4-(3-nitrophenyl)-2-(2-(1-(pyridin-3-yl)ethylidene)hydrazineyl)thiazole</p>

21	 <p>(E)-4-(3-nitrophenyl)-2-(2-(1-(pyridin-4-yl)ethylidene)hydrazineyl)thiazole</p>
22	 <p>(E)-4-(3-nitrophenyl)-2-(2-(1-(pyrazin-2-yl)ethylidene)hydrazineyl)thiazole</p>
23	 <p>(E)-2-(2-((1H-indol-3-yl)methylene)hydrazineyl)-4-(3-nitrophenyl)thiazole</p>
24	 <p>(E)-2-(2-(1-(1H-indol-3-yl)ethylidene)hydrazineyl)-4-(3-nitrophenyl)thiazole</p>
25	 <p>(E)-2-(2-(benzo[d][1,3]dioxol-5-ylmethylene)hydrazineyl)-4-(3-nitrophenyl)thiazole</p>

26	 <p>(E)-2-(2-(1-(benzofuran-2-yl)ethylidene)hydrazineyl)-4-(3-nitrophenyl)thiazole</p>
27	 <p>(E)-2-(2-(1-(2,3-dihydrobenzo[b][1,4]dioxin-6-yl)ethylidene)hydrazineyl)-4-(3-nitrophenyl)thiazole</p>
28	 <p>(E)-2-(2-(naphthalen-1-ylmethylene)hydrazineyl)-4-(3-nitrophenyl)thiazole</p>
29	 <p>(E)-2-(2-(1-(naphthalen-1-yl)ethylidene)hydrazineyl)-4-(3-nitrophenyl)thiazole</p>
30	 <p>(E)-2-(2-(1-(naphthalen-2-yl)ethylidene)hydrazineyl)-4-(3-nitrophenyl)thiazole</p>

31	 <p>(E)-1-(4-(1-(2-(4-(3-nitrophenyl)thiazol-2-yl)hydrazineylidene)ethyl)phenyl)ethan-1-one</p>
32	 <p>2-(2-(diphenylmethylene)hydrazineyl)-4-(3-nitrophenyl)thiazole</p>
33	 <p>(E)-3-(1-(2-(4-(3-nitrophenyl)thiazol-2-yl)hydrazineylidene)ethyl)-2H-chromen-2-one</p>
34	 <p>(E)-4-(3-nitrophenyl)-2-(2-(1-(phenanthren-3-yl)ethylidene)hydrazineyl)thiazole</p>
35	 <p>4-(3-nitrophenyl)-2-(2-(propan-2-ylidene)hydrazineyl)thiazole</p>

36	 <p>1,4-bis((<i>E</i>)-1-(2-(4-(3-nitrophenyl)thiazol-2-yl)hydrazineylidene)ethyl)benzene</p>
37	 <p>(<i>E</i>)-3-(2-(2-(1-(thiophen-2-yl)ethylidene)hydrazineyl)thiazol-4-yl)aniline</p>
Reference	 <p>A complex nucleotide derivative structure featuring a purine base, a ribose sugar, and a phosphate group. The structure is highly detailed, showing the connectivity between the base, sugar, and phosphate, and includes a label 'RLO' at the end of a side chain.</p>

Analysis of molecular docking

PyRx software was used for virtual screening while Discovery Studio 2016 version was used for viewing the interactions between the receptor and ligand. Thirty-seven anti-Parkinson agents were subjected to molecular docking. The molecules were minimized to ensure that the compound fit the side of the active site of the protein in the best conformation. The docking results in binding affinity were spread between -7.3 kcal/mol to -13.6 kcal/mol. A threshold value was fixed as -13 kcal/mol as such, three (3) ligands with a binding affinity above the minimum were selected and studied further. The binding affinity and other parameters were used to screen the 3D conformations of chemical compounds obtained from docking.

Dynamics Simulations

The docking results were valid with the aid of MD simulation [33]. To perform MD simulations, the software called GROMACS 18.1 was utilised [34, 35]. Ligand structure and its topology were assessed via the CHARMM36 force field, and Protein structure and the pdb2gmx module were added [36]. The energy minimization of 5000 steps in a vacuum using the steepest descent method was then performed. Each protein complex was positioned in a box with a distance of 10 Å between the sides. The TIP3P water model was used, with the right ions of sodium and chloride counter ions supplied, the salt concentration of salt [37, 38]. For the simulation, one apo-structure and two protein-ligand complexes were generated. The molecular systems were optimized for the production runs. 100 ns interval simulations were run at a temperature of 310 K and a pressure [39, 40]. XMGRACE software was used for the trajectory plots such as root-mean-square deviation (RMSD), root-mean-square fluctuation (RMSF), radius of gyration (Rg), and solvent accessible-surface-area (SASA), as well as intermolecular hydrogen bonds between the compounds and the protein target [41].

Pharmacokinetics evaluation:

Free online web tools such as swissadme.ch/ and others were consulted to carry out the pharmacological magnitude of the selected ligands [42, 43]. The intended properties were selected to analyze pharmacokinetic, drug-likeness, and physicochemical parameters [44, 45]. In developing desired drug candidates, ADMET evaluation is paramount [46, 47]. The ADMET score is calculated as

$$ADMET\ score = \frac{\sum_{x=1}^z p_i \times y}{\sum_{x=1}^z p_i} \quad \text{Eqn 1}$$

y= transformed result, p= the weight applied to each point, z= number of endpoints

All the top three desired phytochemical properties for both the ligands and referenced drug were examined for drug-likeness. Thereafter, The ADMET properties of the selected ligands were

also analyzed by bringing into play an online free web server [48]. Figure 2 show the overview of the research methodology

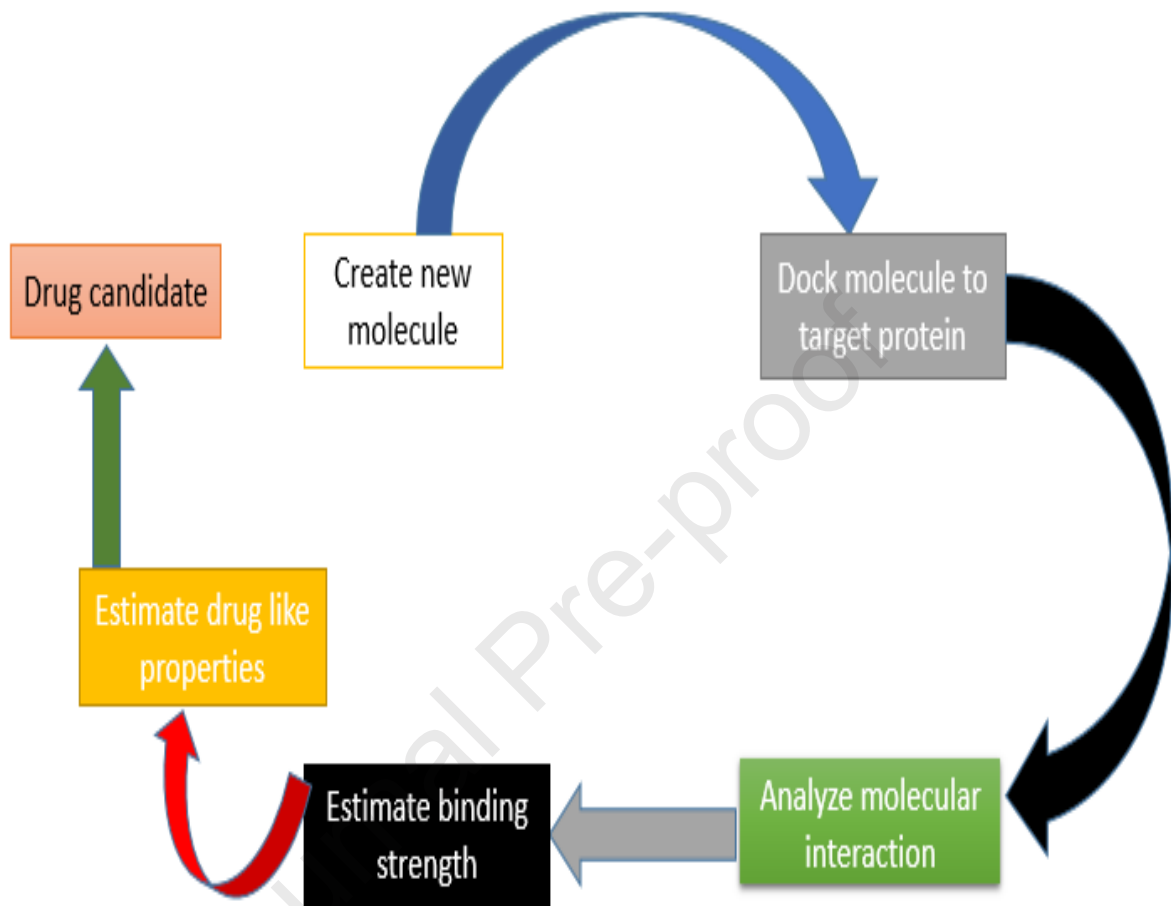


Figure 2: Research methodology

3. Results and Discussion

Molecular Docking

During molecular docking simulation, **Figure 3** shows the region occupied by compound 13 in the protein. All the compounds were found to bind the co-crystal inhibitor ligand (E92602) was bound. Among all the compounds compound 34 was found to have the highest binding affinity (-13.6 kcal/mol) and intermolecular interactions (19). Whereas, the reference was found with the lowest Gibb's free energy (-8.8 kcal mol⁻¹) and interactions (intermolecular) (3). Table 2 shows virtual screening details.

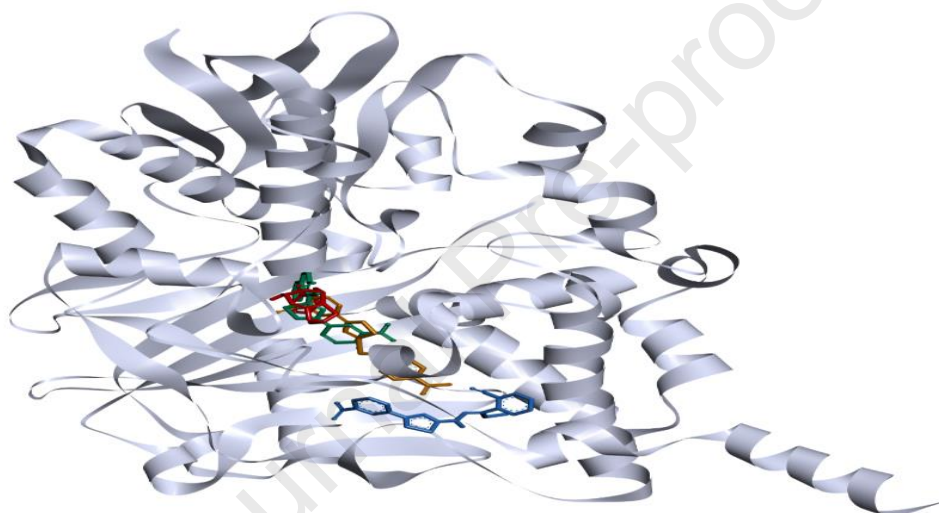


Figure 3: Attachment of the native ligands and reference compound in the protein

Table 2: The receptor and the docked compounds screening

Ligand	Binding affinity (kcalmol ⁻¹)	Bonds no (intermolecular)	Total no. of hydrogen bonds
13	-13.1	8	2
30	-13.3	9	1
34	-13.6	19	9
Reference	-8.8	3	1

According to Reis et al. [30], the binding of the compounds within the inhibitor active site interacts with the key residues like TYR 435, CYS 397, CYS 172, PHE 343, TYR 398, and LYS 296. The binding interactions of the compounds with the amino acid residues of the target protein have been detailed in **Table 3**. Also, the visualization of these interactions has been given in **Figure 4** (3D) and **Figure 5** (2D). In 1 H-pyrrolo-[3, 2-c] quinolones, were evaluated against the human MAO using *in vitro* and *silico* methods [49, 50]. With the compounds showing similar binding

patterns in terms of binding region, our docking results are by [51, 52]. Inhibition of human MAO could be achieved by our compounds [49, 50].

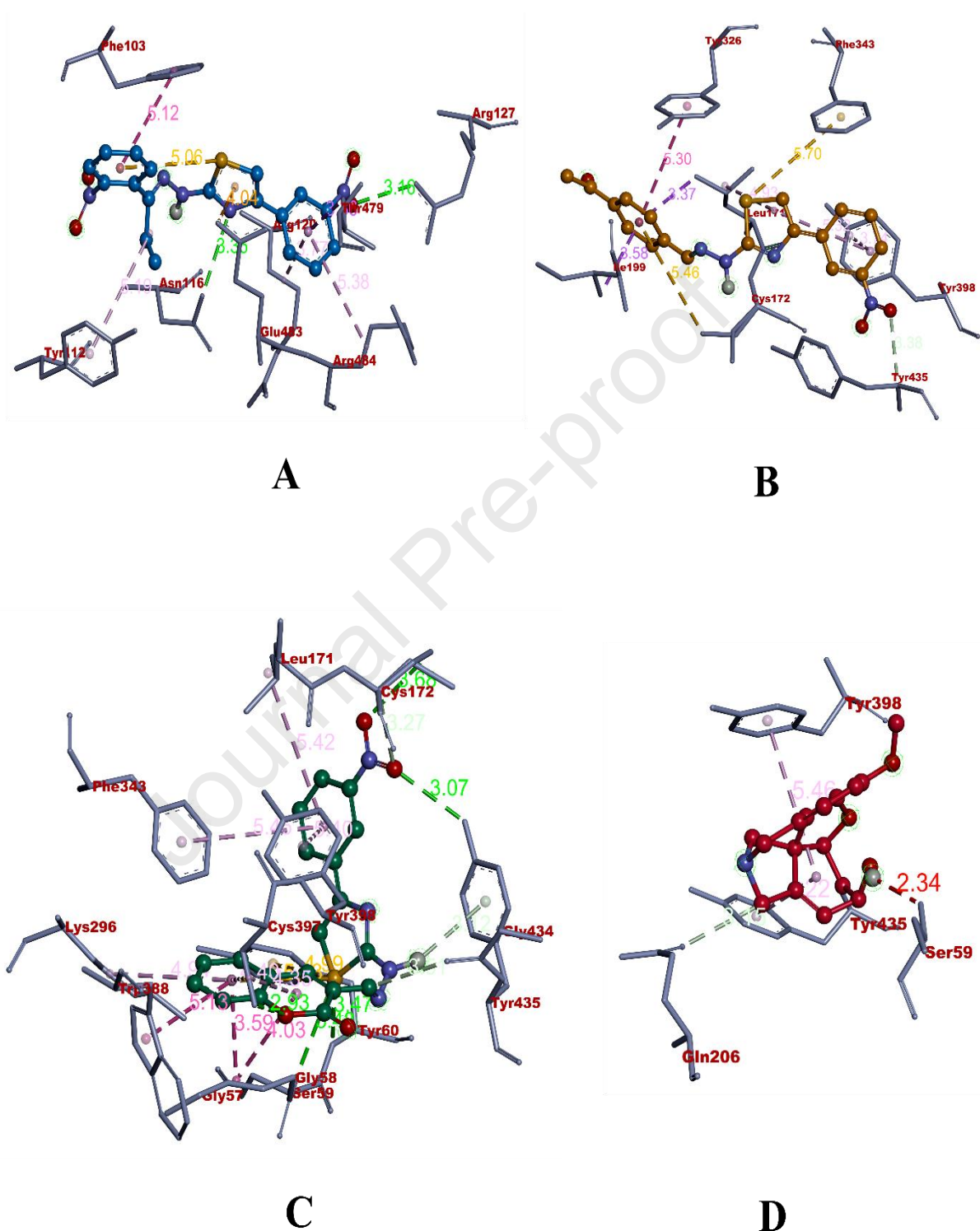


Figure 4: 3D view of: A) compound 13, B) compound 30, C) compound 34, and D) reference.

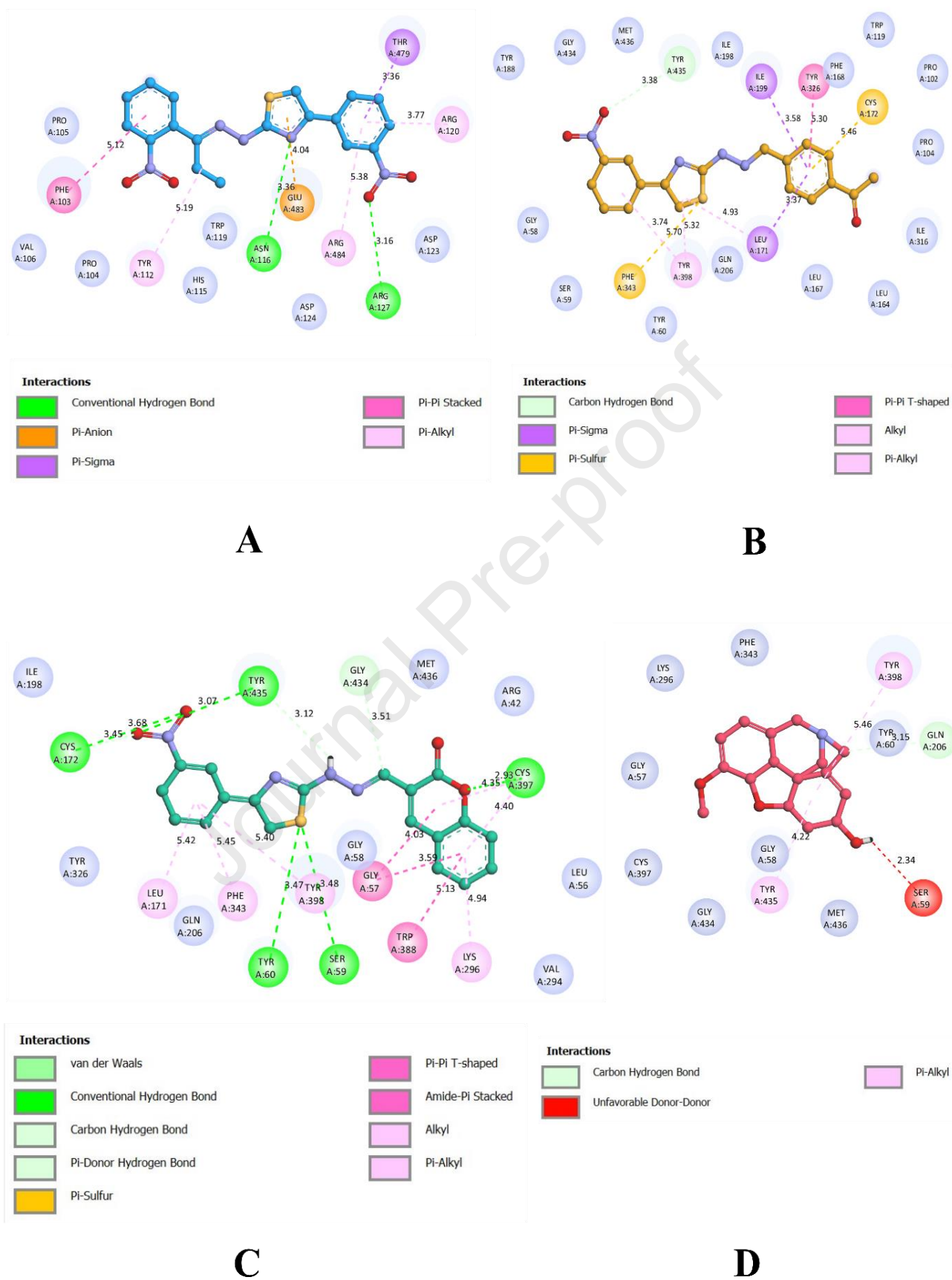


Figure 5: 2D binding interaction view of : A) compound 13, B) compound 30, C) compound 34, and D) reference.

Table 3: Protein interactions with compounds 13, 30, 34, and reference

Ligands	HB	Hydrophobic bonds	
		π - π	π -alkyl
13	ASN116 , ARG127	PHE103	TYR112, ARG120, ARG484
30	TYR 435,	TYR326	TYR398,
34	SER59, TYR60, CYS172 , CYS397, GLY434 , TYR435	TRP388, GLY57,	PHE343, TYR398 LYS296 CYS397
Reference	GLN206	-	TYR398, TYR435

Molecular dynamics (MD) simulation

The degree of stability of the docked complex and the target protein was validated with the aid of MD simulation [53]. Compound 34 and the native ligand trajectories plots are shown in **Figure 6**. The root-mean-square deviation (RMSD) graph depicts the stability of the protein–compound 34 combinations throughout a 100-ns simulation.

It is obvious from Figure 5 that both compound 34 and the reference molecule permanently remained inside the inhibitor binding site. After 10 ns, all of the RMSD plots were stable. Both the protein-compound 34 complex and the apo-protein were on par in the RMSF study, with a nearly identical fluctuating pattern. The C-terminal portion of the protein–reference complex showed a higher number of variations (450-500 residues). Fluctuations between 100–150 and 300–400 residues were also found in the case of the protein-reference drug complex. Higher fluctuations in RMSF plots suggest that the reference drug's inhibitor binding site is unstable.

In addition, Rg and SASA plots were also examined to determine the structural compactness of the generated structures. The Rg plot analysis revealed that the protein-compound 34 complexes remained compact throughout the simulation, resulting in a drop in the SASA value as the ligand occupancy increased. Finally, the complex had changed structurally because of re-arrangement in the ligand.

Furthermore, the ligand RMSD plots reveal that compound 34 was stable inside the inhibitor binding pocket till the simulation completion. But reference drug was highly fluctuating, indicating its instability. The MD simulation outcomes of the compound were by the previous study [54]. Although these researchers have performed the MD simulations for the same protein target, both studies represent the stability only through the RMSD and RMSF plots [54]. Our study, on the other hand, uses GROMACS 18.1 to report on the stability of several plots. The MD simulation results of compound 34 and the reference drug complexed with the protein indicate that both ligands penetrate the inhibitor binding site and form persistent contacts that may contribute to their inhibitory effect. In all of the parameters analyzed for simulation tests, however, compound 34 was determined to be much better than the reference drug. **Table 4** represents the MD trajectory values of compound 34 and reference drug complexed with human MAO.

Table 4: MD trajectory values of compound 33 and reference drug complexed with human MAO.

MD trajectory plots	Apo-protein	Protein-compound 34 complex	Protein-reference complex
RMSD	0.30–0.35 nm	0.30–0.35 nm	0.35-0.40 nm
RMSF (higher fluctuations)	50-100 residues: 0.39 nm	100–150 residues: 0.5 nm, 300-400: 0.42 nm	0-50 residues:0.45 nm
Rg	2.35-2.40 nm	2.40–2.45 nm	2.35-2.40 nm
SASA	220-230 nm ²	230-235 nm ²	220-230 nm ²
Ligand H-bonds	-	10	3
Ligand RMSD	-	0.4-0.5 nm	0.7 nm

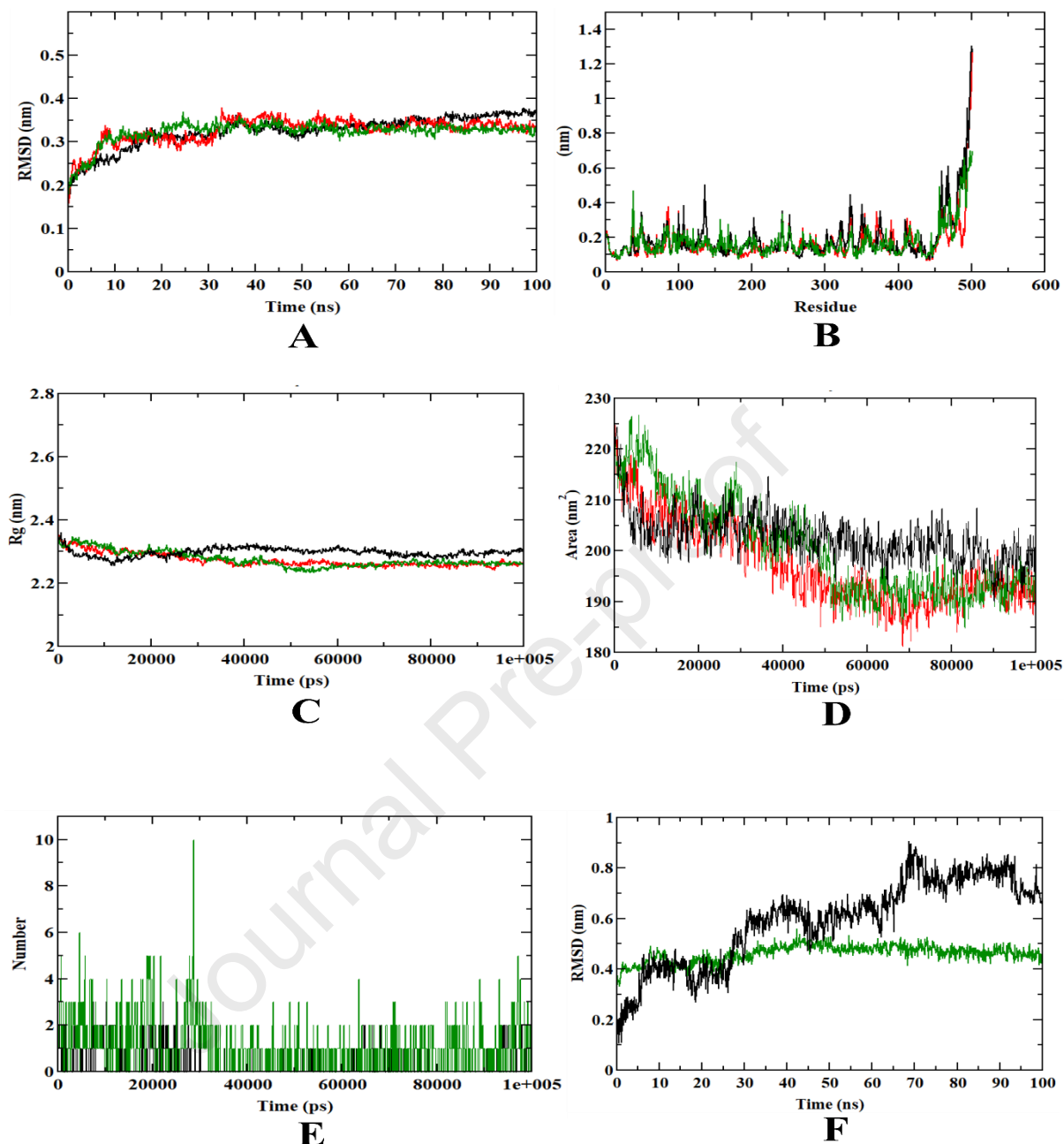


Figure 6: 100 ns trajectories view of MD simulation of MAO B complexed with compound 34 and reference drug. A) target-ligand RMSD, B) target-ligand RMSF, C) target-ligand Rg, D) target-ligand SASA, E) ligand hydrogen bonds, and F) ligand RMSD. Red: apo-protein, green: protein-compound 33 complex, and black: protein-reference drug complex.

Pharmacokinetics assessment

Table 5 shows the pharmacokinetics and drug-likeness parameters of the selected ligands and the referenced drug. The physicochemical and biological properties of the ligands, as well as their drug-likeness, are determined by the ADMET profile analysis using free web-based software. Table 5 shows the predicted drug-likeness, all the molecules were within the threshold value. Human Intestinal Absorption, Caco-2 (colorectal adenocarcinoma cells), Blood-brain barrier, Human oral

bioavailability, Ames mutagenesis, Water-solubility, and Plasma protein binding were the molecular properties predicted for the ligands. As a result, the development and judicious use of new medications necessitate an investigation of their biological activity profiles, which must take into consideration human metabolism [55-57]. As a result of the preceding analysis, it is obvious that the lead-suggested ligands have adequate ability to inhibit the receptor.

Table 5: Drug-likeness *in-silico* prediction.

	13	30	34	REFERENCE
Molecular weight (≤ 500)	397.41	388.44	440.52	287.53
AlogP (< 5)	2.71	4.15	4.27	1.93
HBA (≤ 10)	6	4	4	4
HBD (≤ 5)	1	1	1	1
RTB	7	5	5	1
PSA (≤ 140)	137.16	111.34	111.34	41.93
Linpinski's violation	0	0	0	0
Ghose violations	0	0	0	0
Veber violations	0	0	0	0
Egan violations	0	0	0	0
Muegge violations	0	0	0	0
Bioavailability Scores	0.55	0.55	0.55	0.55
PAINS alert	0	0	0	1
Leadlikeness Violations	0	0	0	2
Synthetic accessibility	3.56	3.47	4.51	4.57
Water solubility	-5.16	-6.14	-6.08	-2.18
Caco2 permeability	0.42	0.39	0.51	-1.04
Intestinal absorption	97.07	91.59	93.12	72.40
Blood-Brain Barrier	-0.78	-0.62	-0.53	0.40
AMES toxicity	No	No	No	Yes
Volume of distribution	1.32	1.28	1.38	0.53

4. Conclusions

PD is an incurable neurodegenerative illness, that mostly affects adults sixty-five years old and above. It gradually leads to an inability to think, reason, learn and imagine things and eventually death. This study used *in-silico* screening, Molecular Dynamics Simulation, and Drug Kinetics Assessment to determine the mechanism of interaction between MAO-B potent inhibitors and protein targets for the treatment of Parkinson's disease by analyzing their binding interactions using molecular simulation and Pharmacokinetic ability. This investigation uncovered three effective therapeutic compounds against the targets (6FW0: 13, 30, and 34). Molecular Dynamics Simulation was

used to better investigate these lead complexes. Throughout the simulation, these complexes maintained stable paths. The ADMET analysis and pharmacokinetic characteristics of the lead compounds also revealed improved drug likeliness. Our findings show that plant-based bioactive compounds have an inhibitory potential against Parkinson's disease and could be used as a medicine to treat the disease.

Acknowledgements: The authors wish to thank the researcher for supporting project RSP 2021/145 at King Saud University Riyadh Saudi Arabia.

Data Availability Statement: All related data are within the manuscript.

Conflicts of Interest: The authors declare no conflict of interest.

References

- Alexander, G. E. (2022). Biology of Parkinson's disease: pathogenesis and pathophysiology of a multisystem neurodegenerative disorder. *Dialogues in clinical neuroscience*.
- Espay, A. J., Vizcarra, J. A., Marsili, L., Lang, A. E., Simon, D. K., Merola, A., & Leverenz, J. B. (2019). Revisiting protein aggregation as pathogenic in sporadic Parkinson's and Alzheimer's diseases. *Neurology*, *92*(7), 329-337.
- Ragab, O. A., Elheneedy, Y. A., & Bahnasy, W. S. (2019). Non-motor symptoms in newly diagnosed Parkinson's disease patients. *The Egyptian Journal of Neurology, Psychiatry and Neurosurgery*, *55*(1), 1-7.
- Schaeffer, E., & Berg, D. (2017). Dopaminergic therapies for non-motor symptoms in Parkinson's disease. *CNS drugs*, *31*(7), 551-570.
- Radhakrishnan, D. M., & Goyal, V. (2018). Parkinson's disease: A review. *Neurology India*, *66*(7), 26.
- Khanfar, M. A., Al-Qtaishat, S., Habash, M., & Taha, M. O. (2016). Discovery of potent adenosine A2a antagonists as potential anti-Parkinson disease agents. Non-linear QSAR analyses integrated with pharmacophore modeling. *Chemico-Biological Interactions*, *254*, 93-101.
- Sebastián-Pérez, V., Martínez, M. J., Gil, C., Campillo, N. E., Martínez, A., & Ponzoni, I. (2019). QSAR Modelling to identify LRRK2 inhibitors for Parkinson's disease. *Journal of Integrative Bioinformatics*, *16*(1).
- R Munteanu, C., Fernández-Blanco, E., A Seoane, J., Izquierdo-Novo, P., Angel Rodriguez-Fernandez, J., Maria Prieto-Gonzalez, J., & Pazos, A. (2010). Drug discovery and design for complex diseases through QSAR computational methods. *Current pharmaceutical design*, *16*(24), 2640-2655.
- Nikolic, K., Mavridis, L., Djikic, T., Vucicevic, J., Agbaba, D., Yelekci, K., & Mitchell, J. B. (2016). Drug design for CNS diseases: polypharmacological profiling of compounds using cheminformatic, 3D-QSAR and virtual screening methodologies. *Frontiers in neuroscience*, *10*, 265.
- De, P., & Roy, K. (2020). QSAR modeling of PET imaging agents for the diagnosis of Parkinson's disease targeting dopamine receptor. *Theoretical Chemistry Accounts*, *139*(12), 1-12.
- Helguera, A. M., Pérez-Garrido, A., Gaspar, A., Reis, J., Cagide, F., Vina, D., & Borges, F. (2013). Combining QSAR classification models for predictive modeling of human monoamine oxidase inhibitors. *European journal of medicinal chemistry*, *59*, 75-90.
- Tong, J. B., Wang, J., Luo, D., Xiao, X. C., Xu, H. Y., Bian, S., & Zhang, X. (2022). QSAR study, molecular docking, and ADMET prediction of vinyl sulfone-containing Nrf2 activator derivatives for treating Parkinson disease. *Structural Chemistry*, *33*(4), 1109-1131.
- Pandey, S., & Srivanitchapoom, P. (2017). Levodopa-induced dyskinesia: clinical features, pathophysiology, and medical management. *Annals of Indian Academy of Neurology*, *20*(3), 190.
- Seppi, K., Ray Chaudhuri, K., Coelho, M., Fox, S. H., Katzenschlager, R., Perez Lloret, S., & Djamshidian-Tehrani, A. (2019). Update on treatments for nonmotor symptoms of Parkinson's disease—an evidence-based medicine review. *Movement Disorders*, *34*(2), 180-198.
- Armstrong, M. J., & Okun, M. S. (2020). Diagnosis and treatment of Parkinson disease: a review. *Jama*, *323*(6), 548-560.
- Tran, T. N., Vo, T. N., Frei, K., & Truong, D. D. (2018). Levodopa-induced dyskinesia: clinical features, incidence, and risk factors. *Journal of Neural Transmission*, *125*(8), 1109-1117.
- Tripathi, A. C., Upadhyay, S., Paliwal, S., & Saraf, S. K. (2018). Privileged scaffolds as MAO inhibitors: Retrospect and prospects. *European Journal of medicinal chemistry*, *145*, 445-497.
- Behl, T., Kaur, I., Sehgal, A., Singh, S., Bhatia, S., Al-Harrasi, A., & Bungau, S. G. (2021). The footprint of kynurenine pathway in neurodegeneration: Janus-faced role in Parkinson's disorder and therapeutic implications. *International Journal of Molecular Sciences*, *22*(13), 6737.

19. Hussain, S., Ullah, F., Ayaz, M., Shah, S.A.A., Shah, S.M., Wadood, A., Aman, W., Ullah, R., Shahat, A.A. and Nasr, F.A., 2019. In silico, cytotoxic and antioxidant potential of novel ester, 3-hydroxyoctyl-5-trans-docosenoate isolated from *anchusa arvensis* (L.) m. bieb. against hepg-2 cancer cells. *Drug Design, Development and Therapy*, 13, p.4195.
20. Er-Rajy, M., Kara, M., Assouguem, A., Belhassan, A., Alotaibi, A., Mrabti, N.N., Fidan, H., Ullah, R., Ercisli, S., Zarougui, S. and Elhallaoui, M., 2022. QSAR, ADMET In Silico Pharmacokinetics, Molecular Docking and Molecular Dynamics Studies of Novel Bicyclo (Aryl Methyl) Benzamides as Potent GlyT1 Inhibitors for the Treatment of Schizophrenia. *Pharmaceuticals*, 15(6), p.670.
21. Khan, A., Pervaiz, A., Ansari, B., Ullah, R., Shah, S.M.M., Khan, H., Saeed Jan, M., Hussain, F., Ijaz Khan, M., Albadrani, G.M. and Altyar, A.E., 2022. Phytochemical Profiling, Anti-Inflammatory, Anti-Oxidant and In-Silico Approach of *Cornus macrophylla* Bioss (Bark). *Molecules*, 27(13), p.4081.
22. Ullah, N., Zeb, S., Rukh, S., Khan, S., Ahmad, I., Ahmad, S., Ahmad, N., Alotaibi, A. and Ullah, R., 2022. Bioassay's Directed Isolation-Structure Elucidation and Molecular Docking of Triterpenes from *Persea duthiei* against Biologically Important Microbial Proteins. *Evidence-Based Complementary and Alternative Medicine*, 2022.
23. Bari, W.U., Zahoor, M., Zeb, A., Khan, I., Nazir, Y., Khan, A., Rehman, N.U., Ullah, R., Shahat, A.A. and Mahmood, H.M., 2019. Anticholinesterase, antioxidant potentials, and molecular docking studies of isolated bioactive compounds from *Grewia optiva*. *International Journal of Food Properties*, 22(1), pp.1386-1396.
24. Shahid, F., Ali, R., Badshah, S.L., Jamal, S.B., Ullah, R., Bari, A., Majid Mahmood, H., Sohaib, M. and Akber Ansari, S., 2021. Identification of Potential HCV Inhibitors Based on the interaction of epigallocatechin-3-gallate with viral envelope proteins. *Molecules*, 26(5), p.1257.
25. Ali, R., Badshah, S.L., Faheem, M., Abbasi, S.W., Ullah, R., Bari, A., Jamal, S.B., Mahmood, H.M., Haider, A. and Haider, S., 2020. Identification of potential inhibitors of Zika virus NS5 RNA-dependent RNA polymerase through virtual screening and molecular dynamic simulations. *Saudi Pharmaceutical Journal*, 28(12), pp.1580-1591.
26. dan, M., Djikic, T., Obradovic, D., & Nikolic, K. (2022). Application of in vitro PAMPA technique and in silico computational methods for blood-brain barrier permeability prediction of novel CNS drug candidates. *European Journal of Pharmaceutical Sciences*, 168, 106056.
27. RaSaini, N., Akhtar, A., Chauhan, M., Dhingra, N., & Sah, S. P. (2020). Protective effect of Indole-3-carbinol, an NF- κ B inhibitor in experimental paradigm of Parkinson's disease: In silico and in vivo studies. *Brain, Behavior, and Immunity*, 90, 108-137
28. Cruz-Vicente, P., Passarinha, L. A., Silvestre, S., & Gallardo, E. (2021). Recent developments in new therapeutic agents against Alzheimer and Parkinson diseases: in-silico approaches. *Molecules*, 26(8), 2193.
29. Patil SM, Martiz RM, Ramu R, Shirahatti PS, Prakash A, Kumar BP, Kumar N (2021a) Evaluation of flavonoids from banana pseudostem and flower (quercetin and catechin) as potent inhibitors of α -glucosidase: an in silico perspective. *J Biomol Struct Dyn* 7:1-5.
30. Reis J, Manzella N, Cagide F, Mialet-Perez J, Uriarte E, Parini A, Borges F, Binda C. Tight-Binding Inhibition of Human Monoamine Oxidase B by Chromone Analogs: A Kinetic, Crystallographic, and Biological Analysis. *J Med Chem*. 2018 May 10;61(9):4203-4212. doi: 10.1021/acs.jmedchem.8b00357. Epub 2018 Apr 20. PMID: 29648817.
31. Ganavi D, Ramu R, Kumar V, Patil SM, Martiz RM, Shirahatti PS, Sathyanarayana R, Poojary B, Holla BS, Poojary, V (2021) In vitro and in silico studies of fluorinated 2,3-disubstituted thiazolidinone-pyrazoles as potential α -amylase inhibitors and antioxidant agents. *Arch Pharm* 12:e2100342
32. Secci, D., Carradori, S., Petzer, A., Guglielmi, P., D'Ascenzio, M., Chimenti, P., & Ortuso, F. (2019). 4-(3-Nitrophenyl) thiazol-2-ylhydrazones derivatives as antioxidants and selective hMAO-B inhibitors: synthesis, biological activity and computational analysis. *Journal of Enzyme Inhibition and Medicinal Chemistry*, 34(1), 597-612.
33. Patil SM, Martiz RM, Ramu R, Shirahatti PS, Prakash A, Chandra JS, Ranganatha LV (2021b) In silico identification of novel benzophenone-coumarin derivatives as SARS-CoV-2 RNAdependent RNA polymerase (RdRp) inhibitors. *J Biomol Struct Dyn* 11:1-17.
34. Poojary B, Kumar V, Arunodaya HS, Chandra S, Ramu R, Patil SM, Baliga A, Rai VM, Vishwanatha U, Vishwanatha P (2021) Potential fluorinated anti-MRSA thiazolidinone derivatives with antibacterial, antitubercular activity and molecular docking studies. *Chem Biodivers* 19:e202100532.
35. Maradesha T, Patil SM, Al-Mutairi KA, Ramu R, Madhunapantula, SV, Alqadi T (2022) Inhibitory effect of polyphenols from the whole green jackfruit flour against α -glucosidase, α -amylase, aldose reductase and glycation at multiple stages and their interaction: Inhibition kinetics and molecular simulations. *Molecules* 27:1888.
36. Gurupadaswamy HD, Ranganatha VL, Ramu R, Patil SM, Khanum SA (2022) Competent synthesis of biaryl analogs via asymmetric Suzuki-Miyaura cross-coupling for the development of anti-inflammatory and analgesic agents. *J Iran Chem Soc* 1:1-16.
37. Martiz RM, Patil SM, Abdulaziz M, Babalghith A, Al-Areefi M, Al-Ghorbani, M, Mallappa Kumar J, Prasad A, Mysore Nagalingaswamy NP, Ramu R (2022a) Defining the Role of Isoeugenol from *Ocimum tenuiflorum* against Diabetes Mellitus-Linked Alzheimer's Disease through Network Pharmacology and Computational Methods. *Molecules* 27:2398.
38. Martiz RM, Patil SM, Ramu R, Jayanthi MK, Ashwini P, Ranganatha LV, Khanum SA, Silina E, Stupin V, Achar RR. (2022b) Discovery of novel benzophenone integrated derivatives as anti-Alzheimer's agents targeting presenilin-1 and presenilin-2 inhibition: A computational approach. *PLoS One* 17:e0265022
39. Kumar V, Ramu R, Shirahatti PS, Kumari VC, Sushma P, Mandal SP, Patil SM (2021) α -Glucosidase; α -Amylase Inhibition; Kinetics and Docking Studies of Novel (2-Chloro-6-(trifluoromethyl) benzyloxy) arylidene Based Rhodanine and Rhodanine Acetic Acid Derivatives. *Chem Select* 6:9637-9644.

40. Kumar V, Shetty P, Arunodaya HS, Chandra KS, Ramu R, Patil SM, Baliga A, Rai VM, Udupi V, Poojary V Poojary B (2022) Potential Fluorinated Anti-MRSA Thiazolidinone Derivatives with Antibacterial, Antitubercular Activity and Molecular Docking Studies. *Chem Biodivers* 19:e202100532
41. Patil SM, Maruthi KR, Bajpe NS, Vyshali VM, Sushmitha S, Chagalamar A, Ramith R (2021c) Comparative molecular docking and simulation analysis of molnupiravir and remdesivir with SARS-CoV-2 RNA dependent RNA polymerase (RdRp). *Bioinformation* 7:932–939.
42. Zhao, Z., Ukidve, A., Kim, J., & Mitragotri, S. (2020). Targeting strategies for tissue-specific drug delivery. *Cell*, 181(1), 151-167.
43. Tiwary, P., Mondal, J., & Berne, B. J. (2017). How and when does an anticancer drug leave its binding site?. *Science advances*, 3(5), e1700014.
44. Nagar, P. R., Gajjar, N. D., & Dhameliya, T. M. (2021). In search of SARS CoV-2 replication inhibitors: Virtual screening, molecular dynamics simulations and ADMET analysis. *Journal of Molecular Structure*, 1246, 131190
45. Mishra, S., & Dahima, R. (2019). In vitro ADME studies of TUG-891, a GPR-120 inhibitor using SWISS ADME predictor. *Journal of drug delivery and therapeutics*, 9(2-s), 366-369.
46. Lucas, A. J., Sproston, J. L., Barton, P., & Riley, R. J. (2019). Estimating human ADME properties, pharmacokinetic parameters and likely clinical dose in drug discovery. *Expert opinion on drug discovery*, 14(12), 1313-1327.
47. Ban, F., Dalal, K., Li, H., LeBlanc, E., Rennie, P. S., & Cherkasov, A. (2017). Best practices of computer-aided drug discovery: lessons learned from the development of a preclinical candidate for prostate cancer with a new mechanism of action. *Journal of chemical information and modeling*, 57(5), 1018-1028.
48. Basu, A., Sarkar, A., & Maulik, U. (2020). Molecular docking study of potential phytochemicals and their effects on the complex of SARS-CoV2 spike protein and human ACE2. *Scientific reports*, 10(1), 1-15.
49. Dhiman P, Malik N, Khatkar A. Lead optimization for promising monoamine oxidase inhibitor from eugenol for the treatment of neurological disorder: Synthesis and in silico based study. *BMC chemistry*. 2019 Dec;13(1):1-20.
50. Grychowska K, Olejarz-Maciej A, Blicharz K, Pietruś W, Karcz T, Kurczab R, Koczurkiewicz P, Doroz-Płonka A, Latacz G, Keeri AR, Piska K. Overcoming undesirable hERG affinity by incorporating fluorine atoms: A case of MAO-B inhibitors derived from 1 H-pyrrolo-[3, 2-c] quinolines. *European Journal of Medicinal Chemistry*. 2022 Jun 5;236:114329.
51. Mateev E, Georgieva M, Zlatkov A. Improved Molecular Docking of MAO-B Inhibitors with Glide. 2022; 13:2, 159.
52. Catalano R, Procopio F, Chavarria D, Benfeito S, Alcaro S, Borges F, Ortuso F. Molecular Modeling and Experimental Evaluation of Non-Chiral Components of Bergamot Essential Oil with Inhibitory Activity against Human Monoamine Oxidases. *Molecules*. 2022 Apr 11;27(8):2467.
53. Santos, L.H.S.; Ferreira, R.S.; Caffarena, E.R. Integrating Molecular Docking and Molecular Dynamics Simulations. *Methods. Mol. Biol.* 2019, 2053, 13-34.
54. Chaurasiya ND, Zhao J, Pandey P, Doerksen RJ, Muhammad I, Tekwani BL. Selective inhibition of human monoamine oxidase B by acetin 7-methyl ether isolated from *turnera diffusa* (Damiana). *Molecules*. 2019 Jan;24(4):810.
55. Abdalla, M. A., Li, F., Wenzel-Storjohann, A., Sulieman, S., Tasdemir, D., & Mühlhling, K. H. (2021). Comparative metabolite profile, biological activity and overall quality of three lettuce (*Lactuca sativa* L., Asteraceae) cultivars in response to sulfur nutrition. *Pharmaceutics*, 13(5), 713.
56. Olasupo, S. B., Uzairu, A., Shallangwa, G. A., & Uba, S. (2021). Computer-aided drug design and in silico pharmacokinetics predictions of some potential antipsychotic agents. *Scientific African*, 12, e00734.
57. Olasupo, S. B., Uzairu, A., Shallangwa, G. A., & Uba, S. (2021). Unveiling novel inhibitors of dopamine transporter via in silico drug design, molecular docking, and bioavailability predictions as potential antischizophrenic agents. *Future Journal of Pharmaceutical Sciences*, 7, 1-10.

The authors gratefully acknowledged the technical effort of Dr. Abdulfatai Usman, Dr Stephen Ekeh and Dr Samuel Adawara all of chemistry department, Ahmadu Bello University, Zaria.

Journal Pre-proof

Data availability

- <https://doi.org/10.1080/14756366.2019.1571272>

Journal Pre-proof

Declaration of interest statement

The authors declare that they have no competing interests

Journal Pre-proof